

Modelocked Lasers and Ultrashort Pulses

Modelocking of Lasers to Produce Ultrashort Pulses has Opened New Research Areas

by Bernard Couillaud and Vittorio Fossati-Bellani

This article is not a review article on the present status of modelocking operation of lasers. Rather, it's an introduction to ultrafast phenomena, intended for readers unfamiliar with the field. We have restricted ourselves to the modelocking operation of continuouswave sources, particularly the cw dye laser, because of its capability to generate the shortest pulses available at present.

Basics of Modelocking

A laser is an optical oscillator, generally consisting of an amplifier medium within an optical cavity acting as a feedback loop. An oscillation takes place within the laser cavity when the usual conditions for oscillation — unsaturated gain larger than intracavity losses and phase self-consistency over a round trip — are fulfilled. The latter condition expresses the fact that the phase of the optical radiation must be identically reproduced after a round trip, within an integer number of 2π . It shows that only those frequencies,

ν , corresponding to the resonance frequencies of the optical cavity defined by $\nu = kc/2L$ (k is an integer, c is the speed of light, and L is the optical length of the resonator) are susceptible to oscillate. The actual oscillating frequencies are those frequencies resonant in the laser cavity for which the unsaturated gain is larger than the intracavity losses. These oscillating frequencies are the axial modes of the laser.

An optical oscillator, as described above, can operate in three different regimes. These regimes are referred to as multimode, single frequency, and modelocked.

Multimode operation of a laser corresponds to the situation where more than one axial mode is oscillating within the laser cavity. The phase of each of these modes varies randomly with time. Most lasers are naturally multimode in their basic configurations. Single frequency operation describes an oscillator where all the axial modes but one have been suppressed, generally by using intracavity filters. The resultant high monochromaticity has been the origin, during the past 15 years, of the revolution in frequency domain spectroscopy.

While multimode and single frequency operation of lasers are common knowledge, the third mode of operation, modelocking (or, as it

is sometimes called, phaselocking) is generally less known among laser users.

To give a very simplified picture of modelocking operation, let's

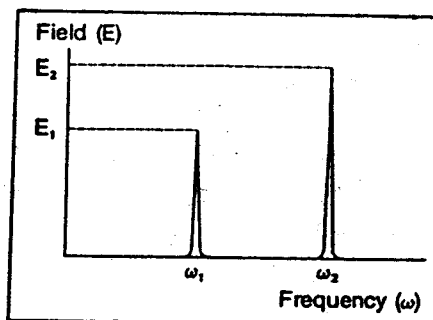


Figure 1. Spectral amplitude distribution for a laser with two axial modes.

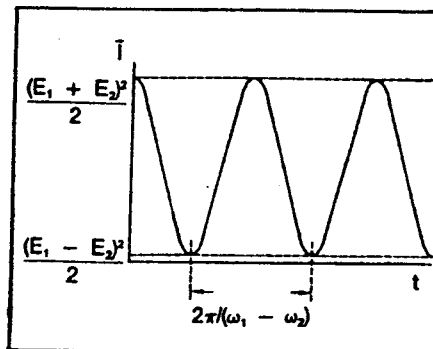


Figure 2. Output of a laser with constant phases of two axial modes.

Bernard Couillaud, on leave from the University of Bordeaux, is department head of dye laser engineering and Vittorio Fossati-Bellani is product manager of ultrafast laser systems at Coherent Inc., Palo Alto CA.

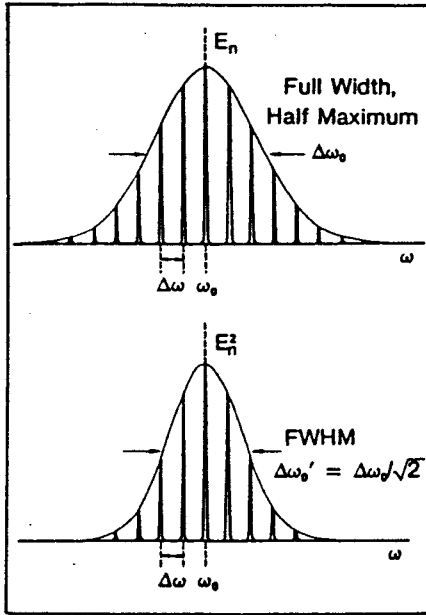


Figure 3. Gaussian spectral amplitude distribution and corresponding spectral intensity.

consider a laser oscillating over two axial modes only (Figure 1). Throughout this article, we assume all oscillations are in the fundamental transverse mode only. The transverse modelocking that could result from coupling between axial modes related to different transverse modes will not be considered.¹ The two oscillations are assumed linearly polarized along the same direction, so that a scalar description can be used. The electric fields describing each of the two oscillating radiation modes will be

$$E_1 = E_1 \cos(\omega_1 t + \phi_1(t)) \quad (1)$$

and

$$E_2 = E_2 \cos(\omega_2 t + \phi_2(t)) \quad (2)$$

This treatment assumes a temporal dependence of the phases ϕ_1 and ϕ_2 .

A detector probing the laser output gives a signal proportional to the square of the electric field. Thus,

$$I = (E_1 + E_2)^2 = E_1^2 \cos^2(\omega_1 t + \phi_1(t)) + E_2^2 \cos^2(\omega_2 t + \phi_2(t)) + 2E_1 E_2 \cos(\omega_1 t + \phi_1(t)) \cos(\omega_2 t + \phi_2(t)) \quad (3)$$

In fact, every actual detector has a response time, τ , much larger than the optical period of oscillation. Thus, the detector's output signal is proportional to the mean value, \bar{I} of I over the time, τ , is given by

$$\bar{I} = \frac{E_1^2}{2} + \frac{E_2^2}{2} + \frac{E_1 E_2}{\tau} \int_0^\tau \cos[(\omega_1 - \omega_2)t + (\phi_1(t) - \phi_2(t))] dt \quad (4)$$

In Eq. 4, the first two terms are the contributions to the signal given by each mode considered separately. The third term expresses the interference occurring between the two oscillations.

If the phases $\phi_1(t)$ and $\phi_2(t)$ are randomly varying with time, with a characteristic time much shorter than the response time of the detector, τ , then the interference term averages to zero even if a fast detector [$2\pi/\omega_0 < \tau < 2\pi/(\omega_1 - \omega_2)$] is used. This situation corresponds to the multimode operation (2 modes in this case) characterized by a laser output intensity constant over time.

Now let's suppose that, through means to be discussed later, we can "freeze" the phases ϕ_1 and ϕ_2 , thus suppressing their time dependence. If the detector's response time is smaller than $2\pi/(\omega_1 - \omega_2)$, the signal exhibits a sinusoidal modulation at frequency $(\omega_1 - \omega_2)/2\pi$, as shown in Figure 2. By freezing the phases of the two axial modes, we have succeeded in changing the time dependence of the laser output.

Using this simplified two-mode picture, we have reinvented the beat frequency: When the frequencies of the two modes are perfectly defined, a beating term at the difference frequency modulates the laser intensity. In our particular case, where the interference involves only two waves, the time dependence of the beating is sinusoidal.

Generally, though, a laser output exhibits many axial modes. Here, the phase-freeze condition, corresponding to modelocking, produces a multiple interference term to replace the two-wave interference term of the two-mode model.¹ To better understand the consequences of multiwave interference, let's consider the case of a laser output consisting of an infinite number of axial modes, with a Gaussian distribution of the mode amplitude centered at ω_0 (Figure 3). The amplitude of the field describing each mode is then

$$E_n = E_0 \exp\left[-\left(\frac{2n\Delta\omega}{\Delta\omega_0}\right)^2 \text{Log}2\right] \quad (5)$$

where E_0 is the field amplitude for the mode at ω_0 , n is the mode number counted from ω_0 , $\Delta\omega = c/2L$ is the intermode spacing, and $\Delta\omega_0$ is the full width at half maximum (FWHM) of the field distribution. In an ideal situation where the phases of the different modes are frozen at $\phi_n = 0$, the total electric field becomes

$$E(t) = \sum_{n=-\infty}^{+\infty} E_n \exp j\omega_n t \quad (5a)$$

which can be written

$$E(t) = \exp j\omega_0 t \sum_{n=-\infty}^{+\infty} E_n \exp(jn\Delta\omega t) \quad (6)$$

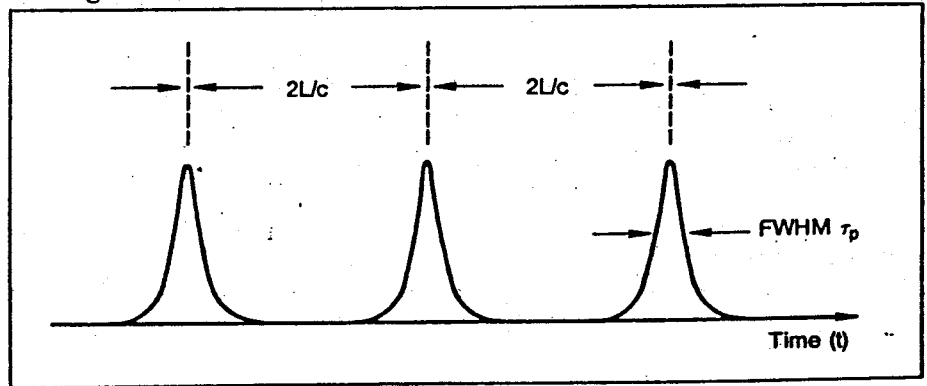


Figure 4. Time behavior of the output intensity of a modelocked laser characterized by a Gaussian spectral amplitude distribution.

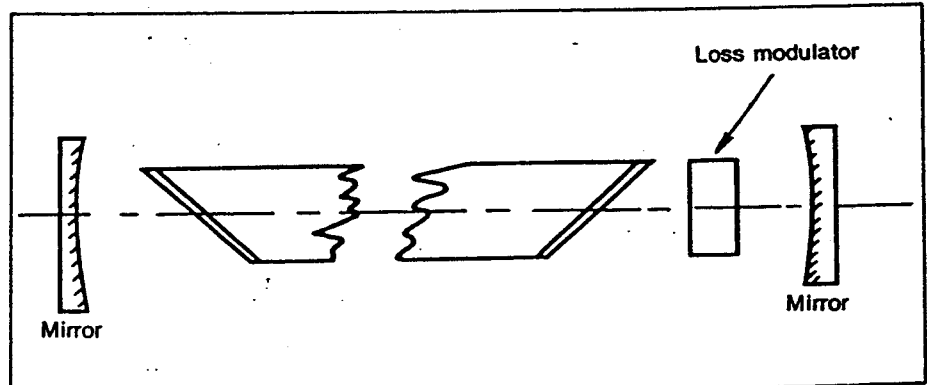


Figure 5. Schematic of an actively modelocked laser.

where the relation $\omega_n = \omega_0 + n\Delta\omega$ has been used. The total field $E(t)$ consists of a carrier wave at optical frequency ω_0 , modulated by a slowly variable function of time, $k(t)$, defined by

$$k(t) = \sum_{n=-\infty}^{+\infty} E_n \exp(jn\Delta\omega t) \quad (7)$$

Since the right part of Eq. 7 corresponds to the Fourier transform of $k(t)$, $k(t)$ is a periodic function of time, with a period $T = 2\pi/\Delta\omega = c/2L$. This periodic behavior is characteristic of the laser intensity when probed with a fast detector, τ is much less than $2\pi/\Delta\omega$. Another characteristic of the laser output can be obtained from the spectral amplitude distribution given in Eq. 5. By Fourier theory, if the E_n have a Gaussian distribution, $k^2(t)$ will exhibit a Gaussian shape in time (Figure 4). Approximating the sum in Eq. 7 by an integral over n , one finds that

$$k^2(t) \propto \exp\left[-\left(\frac{2t}{\tau_p}\right)^2 \text{Log}_N 2\right] \quad (8)$$

where τ_p , the pulse duration (FWHM), is given by

$$= \frac{2\sqrt{2}}{\pi\Delta\omega_0} \text{Log}_N 2 \quad (9)$$

Thus, for perfect modelocking where the spectral amplitude distribution has been chosen as Gaussian, the laser output consists of an infinite train of Gaussian-shaped light pulses separated in time by $2L/c$. The periodic behavior of the laser output is solely due to the equal intermode spacing of the axial modes and is independent of the amplitude distribution. This behavior is often visualized by imagining a pulse travelling within the laser cavity, losing part of its energy through the output coupler at every round trip.

Eq. 9 shows that the pulse duration is inversely proportional to the FWHM of the spectral amplitude distribution. Thus, lasers presenting the largest emission bandwidth will provide the shortest pulses, a fact that explains the extensive use of modelocked dye lasers in studies of ultrafast phenomena.

Eq. 9 relates τ_p and $\Delta\omega_0$ for a Gaussian amplitude distribution. If a different distribution were chosen, a similar expression would be found.

The proportionality factor $(2\sqrt{2}/\pi)(\text{Log}_N 2)$ would be changed. But the proportionality factor would remain of the order of one. A pulse is called Fourier-transform limited

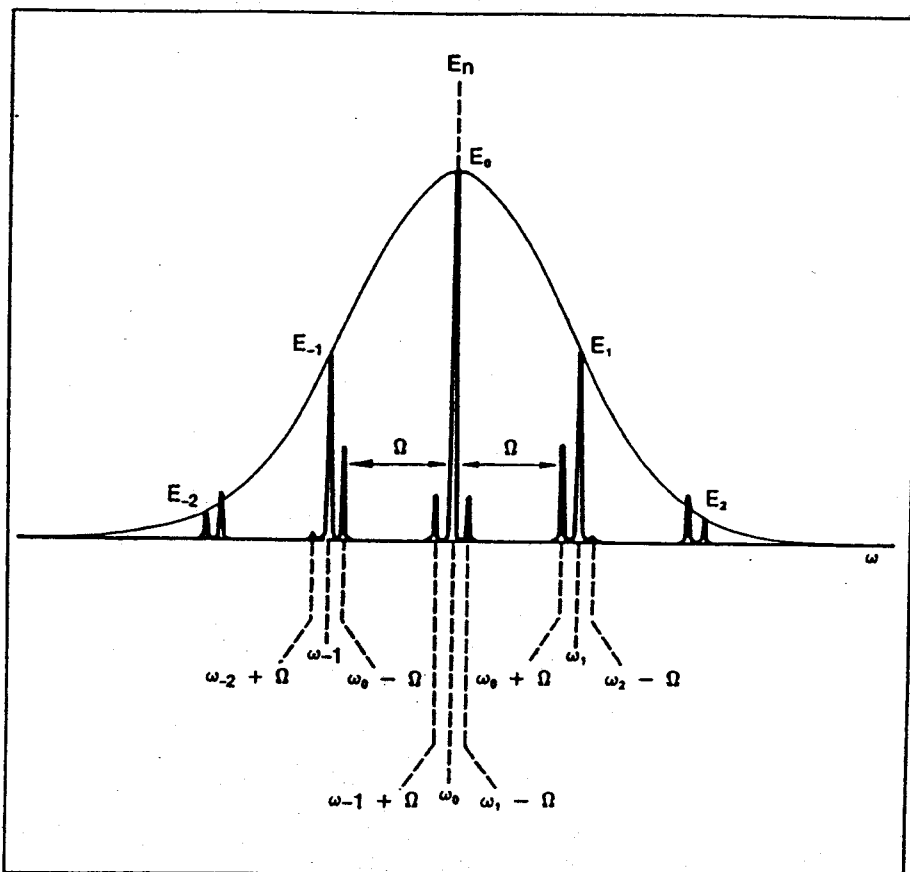


Figure 6. Generation of side bands in amplitude modulation (AM) modelocking. ω_n are the laser's axial modes and Ω is the amplitude modulation frequency.

(or, more colloquially, transform-limited) when τ_p and $\Delta\omega_0$ obey a relation like Eq. 9, including the proper proportionality factor.

To check if a pulse is transform-limited, τ_p can be measured with a fast photodiode, a streak camera, or an autocorrelator. The width of the spectral distribution can be measured with a spectrograph or a Fabry-Perot interferometer. In both cases, since the detector used is quadratic, the instrument will display the intensity spectral distribution. The relation between $\Delta\omega_0$ and the FWHM $\Delta\omega_0'$ of the experimental curve depends on the shape of the distribution. It is given by $\Delta\omega_0' = \Delta\omega_0/\sqrt{2}$ for a Gaussian profile (Figure 3).

A large discrepancy between an experimentally derived $\Delta\omega_0$ and the $\Delta\omega_0$ calculated from Eq. 9 (or a similar expression, if non-Gaussian) is evidence of imperfect modelocking. The laser output will still be a recurrent train of pulses, but the carrier frequency (ω_0 in Eq. 6) will sweep the experimental frequency range $\Delta\omega_0$.

For perfect modelocking, knowledge of the spectral amplitude distribution (Eq. 5) is equivalent to the knowledge of the field amplitude function, $k(t)$, since a simple mathematical transformation calculates one from the other. Consequently, the description of a given mode-

locked situation can be carried out in either the frequency or time domains, without altering its validity.

Defining Active and Passive Modelocking

Lasers generally operate in the multimode regime, although nonlinear interactions within the lasing medium can lead to "self locking" of the phases.² The production of very short optical pulses by means of laser modelocking requires the insertion of an external element into the laser resonator. The external element initiates and maintains the proper coupling between the axial modes. If the modelocking device must be driven by a source of energy external to the laser, the method is called active modelocking. If no other energy than the energy available in the laser oscillator is required, the method is called passive modelocking.

Each of the atoms or molecules in the lasing medium in the upper state of the relevant laser transition can participate in the amplification of the light travelling back and forth in the optical resonator. Each atom or molecule has a given potential emission bandwidth, based on such factors as the finite lifetime of the upper state for an atomic medium or the wide spread of energy available

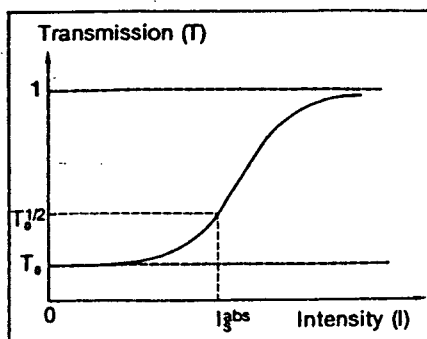


Figure 7. Transmission versus incident power for a saturable absorber.

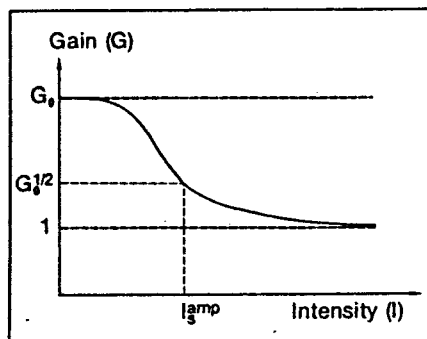


Figure 8. Gain versus power for an amplifier medium.

in the lower singlet state of dye molecules. (For simplicity, we disregard the inhomogeneous broadening that could result, for example, from a Doppler effect in a gaseous medium.³) This bandwidth is generally much larger than the laser intermode spacing, $c/2L$, so neighboring axial modes compete with each other for gain. This situation is typical of the multimode operation of lasers, where the mode competition induces large fluctuations of the phases and amplitudes of the oscillating axial modes.

Active Modelocking

Let's put an element that periodically modulates the laser intracavity losses into our laser oscillator (Figure 5). Since the action of this element is more readily understood in the frequency domain, we consider the effect of an amplitude modulation on the laser's amplitude spectral distribution. The modulation losses within the laser cavity result in an amplitude modulation of each axial mode. If the modulation is assumed sinusoidal with a circular frequency, Ω , and a modulation index, α , the time dependence of the mode n at frequency ω_n can be written

$$\epsilon_n(t) = E_n \cos(\omega_n t + \phi_n) [1 - \alpha (1 - \cos(\Omega t + \phi))] \quad (10)$$

If viewed in the frequency domain, the amplitude modulation corre-

sponds to the creation of two side bands, as can be easily shown by rearranging $E_n(t)$ to obtain (Figure 6)

$$\begin{aligned} \epsilon_n(t) = & E_n(1 - \alpha)\cos(\omega_n t + \phi_n) \\ & + E_n \frac{\alpha}{2} [\cos\{(\omega_n - \Omega)t + \phi_n - \phi\} \\ & - \cos\{(\omega_n + \Omega)t + \phi_n + \phi\}] \quad (11) \end{aligned}$$

If the modulation frequency, $\Omega/2\pi$, is set equal to the laser intermode spacing, $c/2L$, the two side bands of a given axial mode are located on each side of the mode, at the next-neighbor mode frequency. (An amplitude modulation frequency at $mc/2L$, where m is an integer, can also be used.⁵) The side bands and the axial modes compete for gain within the laser medium. Instances where the axial modes lock their phases to the corresponding side bands, resulting in a complete phase freeze in the amplitude spectral distribution, correspond to the most efficient use of the lasing medium. This determines the conditions that "win" the competition for gain. As a result of this phase locking, the oscillating modes interfere to produce a continuous train of short light pulses. This technique, referred to as amplitude modulation (AM) modelocking,^{6,7} is used for ion or Nd:YAG laser oscillators where an acousto-optic modulator is inserted inside the optical resonator to modulate the intracavity losses. Modelocking can be obtained through

frequency modulation (FM), as well.^{8,9,10} Since some radio-frequency power is needed to drive the modulator, these techniques belong to the domain of active modelocking.

Modelocking can also be achieved by modulating the laser gain rather than the losses. In the case of cw dye lasers that need to be pumped by another laser (ion or Nd:YAG), this situation is commonly achieved by pumping with a modelocked laser and adjusting the length, L , of the dye laser cavity, so that its pulse repetition rate is equal to that of the pump laser. We will discuss such synchronous pumping in an upcoming section.

Passive Modelocking

Passive modelocking techniques^{11,12} generally use a nonlinear absorber (usually a solution of organic dyes) inserted within the laser cavity.

Consider the transmission characteristics of a saturable absorber. At low incident power, the absorber's transmission is constant, almost independent of the incident power. As the incident power continues to increase, however, the population of the upper state involved in the absorption process and the stimulated emission probability from this level are increased, while the lower state population is decreased. The combination of these processes leads to a

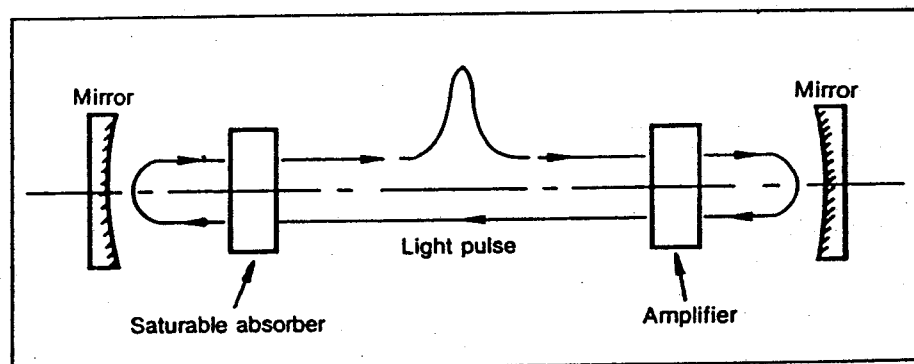


Figure 9. Schematic of a passively modelocked laser.

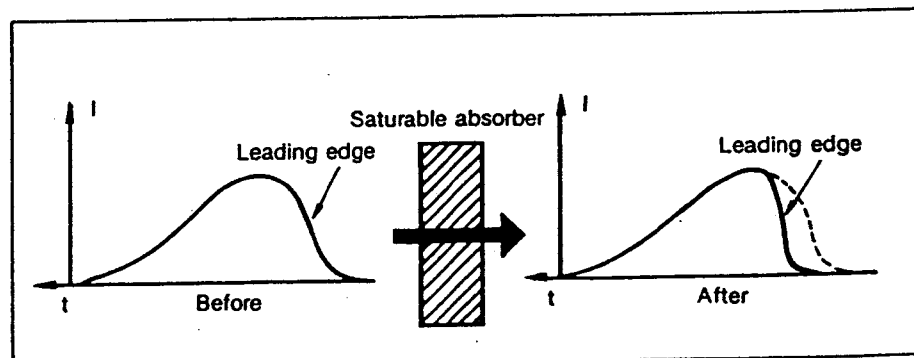


Figure 10. Interaction of a short pulse with a saturable absorber.

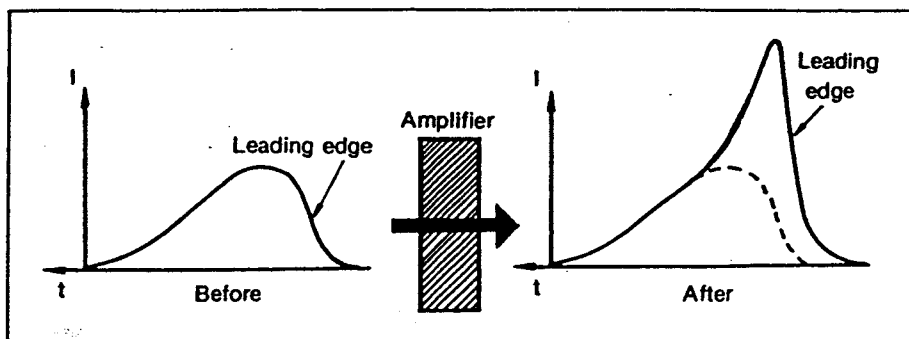


Figure 11. Interaction of a short pulse with an amplifier medium.

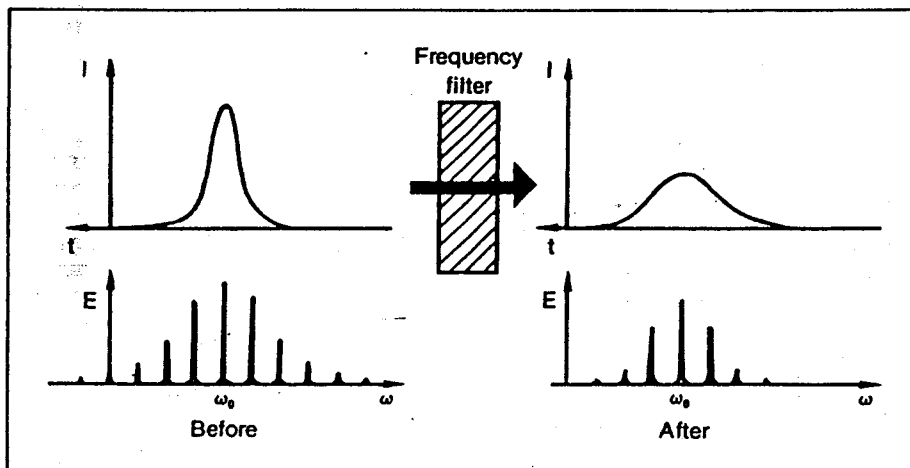


Figure 12. Interaction of a short pulse with a frequency filter.

transmission that increases nonlinearly with the input power, as depicted in Figure 7. Saturable absorbers are often characterized by a quantity called the saturation intensity, I_s^{abs} . This quantity is defined as the intensity required to decrease by one-half the population difference existing under small-signal excitation between the two levels involved in the absorption process. This definition relates directly to the absorption coefficient of the medium, because this coefficient is proportional to the population difference encountered.

Similarly, a gain medium presents some saturation properties, too. At low input power, the gain is called unsaturated and presents its largest value. When the input power is increased, the inversion of population existing between the levels involved in the amplification process decreases, and so does the gain. Figure 8 depicts a typical variation of gain in an amplifier medium versus input power. As with the saturable absorber, saturation intensity, I_s^{amp} , is defined by changing "absorption" to "amplification" in the preceding paragraph.

We can describe, in the time domain, how a pulse is formed in a passively modelocked laser¹³ by using these concepts. The laser consists of an amplifier and a saturable

absorber placed within an optical resonator (Figure 9). At the beginning, the intracavity power is null, and the unsaturated gain is larger than the sum of the optical resonator losses. A quasi-cw oscillation can then take place, where, during the early stage of the laser action, the radiation field in the laser cavity consists of many irregular fluctuations of low power. As the power builds up, the peak intensity of the highest fluctuation starts to bleach the absorber. This particular fluctuation then experiences lower losses than the smaller fluctuations, causing it to grow more quickly than its smaller brethren. This growth allows it to consume a disproportionate share of the available gain, thereby starving its smaller brethren. Eventually, one big pulse will collect all the energy.

Now let's follow the pulse during one round trip within the optical resonator. Let's start with the early formation of the pulse, when it has already been formed but before it has reached its final shape and duration. As the pulse crosses the saturable absorber, where lower powers are more readily absorbed than higher powers, the *leading edge* of the pulse is significantly absorbed (Figure 10). But the peak of the pulse bleaches the absorber. If the absorber's recovery time is longer than

the pulse duration, as is common with dye lasers, the *trailing edge* of the pulse will see the transparency caused by the peak of the pulse and will be unattenuated.

When the pulse reaches the amplifier medium, the *leading edge* experiences an unsaturated gain and is largely amplified, while the *trailing edge* is left with highly saturated gain and is much less amplified (Figure 11). Thus, a narrow pulse with high peak power can be created in the laser cavity, if a portion of the evolving pulse is untouched by the absorber and amplified by the amplifier medium. This will occur as long as the saturable absorber saturates more quickly than the amplifier medium.

The ultimate pulse shape is obtained in the system when a steady-state, corresponding to the self-consistency of the optical pulse within the laser cavity, is reached. This self-consistency expresses the fact that the pulse should reproduce itself identically after a round trip. The discussion in the preceding two paragraphs might suggest that pulses would tend to become infinitely narrow. But they don't. As was noted earlier, the duration of the pulse, under perfect modelocking conditions, is inversely proportional to the width of the spectral amplitude distribution. So, any "element" within the cavity restricting the oscillating bandwidth of the laser acts as a broadening device. The element can be an optical component external to the amplifier medium, such as a prism, grating, or Lyot filter. Or the amplified medium itself may provide broadening.

The broadening effect can be most readily explained by referring to the picture in the frequency domain.¹³ Before entering the filtering element, the optical pulse is described by its spectral amplitude distribution. The frequency-dependent transmission of the filter (itself related to the optical cavity and gain medium parameters) alters the spectral amplitude distribution by decreasing the wing amplitudes, while leaving the central part basically unchanged. The narrowing of the spectral amplitude distribution explains the broadening in time experienced by an optical pulse crossing a filtering element (Figure 12). Similarly, any intracavity dispersive element will also act as a pulse resaper, by delaying the different frequency components of the spectral amplitude distribution.

Synchronous Modelocking

Figure 13 shows the general schematic of a synchronously pumped modelocked system. It involves two lasers. The first laser, used to pump the amplifier medium of the second laser, is a modelocked laser generating a continuous train of pulses at repetition rate $c/2L_1$, where L_1 is the optical length of the first laser's resonator. The second laser, with a resonator optical length L_2 , uses an amplifier medium characterized by a recovery time shorter than the time interval $2L_1/c$ existing between two consecutive pulses of the pump laser. Under the pump excitation, the gain of the second laser is then modulated at the frequency $c/2L_1$. The second laser will operate in a modelocking regime, if its intermode spacing, $c/2L_2$, is adjusted to the frequency of the gain modulation, $c/2L_1$. This condition can be achieved by forcing the length of the two laser cavities to be equal.

For simplicity, we will restrict ourselves to the discussion of the most common system presently used, a modelocked argon-ion or frequency-doubled Nd:YAG laser, synchronously pumping a cw dye laser. The widespread interest in such a combination stems from the characteristics of dye lasers. With a gain bandwidth of the order of 50 nanometers, dye lasers can provide widely tunable picosecond and subpicosecond pulses. In comparison, the narrow linewidth of the pump laser ($\sim 10^{-2}$ nm) limits the pump laser duration to about 100 ps.

To study pulse-shape evolution in the dye laser with length detuning, let's suppose that a steady-state regime has been obtained: A narrow pulse is travelling within the dye laser's optical cavity. The oscillation conditions require that the dye pulse crosses the amplifier medium when the gain induced by the pump pulse is larger than the intracavity losses. Figure 14 gives a schematic of the variation of the gain due to the passing of the pump and dye pulses through the dye amplifier medium. The horizontal axis is in arbitrary units of time at the dye medium. At $t = 0$, the pump pulse arrives at the amplifier medium, pumping the dye molecules to the excited state. The gain builds up following the integral of the pump pulse intensity, until the dye pulse travelling within the cavity reaches the dye amplifier. At this time, a loss of population inversion due to the stimulated emission caused by the dye pulse is induced

in the medium. This loss of population shows as a sharp dip in the gain curve at exactly the same time that the dye pulse strikes the amplifier. While the gain drops below the level of the intracavity losses, the long duration of the pump pulse allows the gain to build up again after the dye pulse has passed.

What does length mismatching do to the dye laser output? Remember, the round trip time of the dye pulse within the dye optical resonator is fixed by the repetition rate of the pump pulse. The resulting length matching between the two laser cavities is then rather critical. However, pulse reshaping in the amplifier medium will automatically compensate for small induced changes in the round trip propagation time, so length mismatches on the order of 100 micrometers can be tolerated without destroying stable operation in the system.

This reshaping process can be qualitatively explained by considering the saturation of the gain induced by the dye pulse in the amplifier medium. Before the pulse arrival, the gain is unsaturated. Thus, the leading edge of the pulse experiences a larger gain than the trailing edge. This preferential amplification of the leading edge of the pulse produces a new pulse that is slightly advanced, so the transit time of the pulse across the amplifier medium is shortened. The advance experienced by the dye pulse in the amplifier medium is directly related to the value of the unsaturated gain at the crossing time and occurs regardless of the laser cavity length permitting a stable operation. In particular, this reshaping effect explains the slight positive length mismatch ($L_2 = L_1$

+ ϵ) that characterizes the perfect modelocking operation in synchronously pumped systems.¹⁶

Now let's shorten the dye laser cavity slightly from its optimum length. The dye pulse circulating within the optical resonator will arrive at the amplifier medium earlier than would be optimum. Since the value of the unsaturated gain is proportional to the integral of the pump pulse over time, the leading edge of the dye pulse experiences lower gain than in the optimum position. The corresponding decrease in the efficiency of the reshaping process produces an increase in the effective transit time through the amplifier medium. A new steady state, involving a new pulse shape for which the pulse advance induced by the cavity shortening is cancelled by the increase in the amplifier transit time, can then take place in the dye amplifier.

The same sort of argument can be made regarding a lengthening of the laser cavity. Here, the dye pulse is retarded by the longer cavity and arrives at the dye later than optimum. But it sees higher unsaturated gain than optimum, so its transit time through the amplifier medium is reduced accordingly.

Thus, slight changes of the dye laser cavity during stable operation induce a readjustment of the dye pulse shape. Many of the features of the pulse dependence on cavity length detuning can be explained qualitatively from the model for gain evolution shown in Figure 14. The autocorrelation traces of pulses obtained for different settings of the dye laser cavity length are given in Figure 15. Figure 15b is the trace of the pulse shape corresponding to

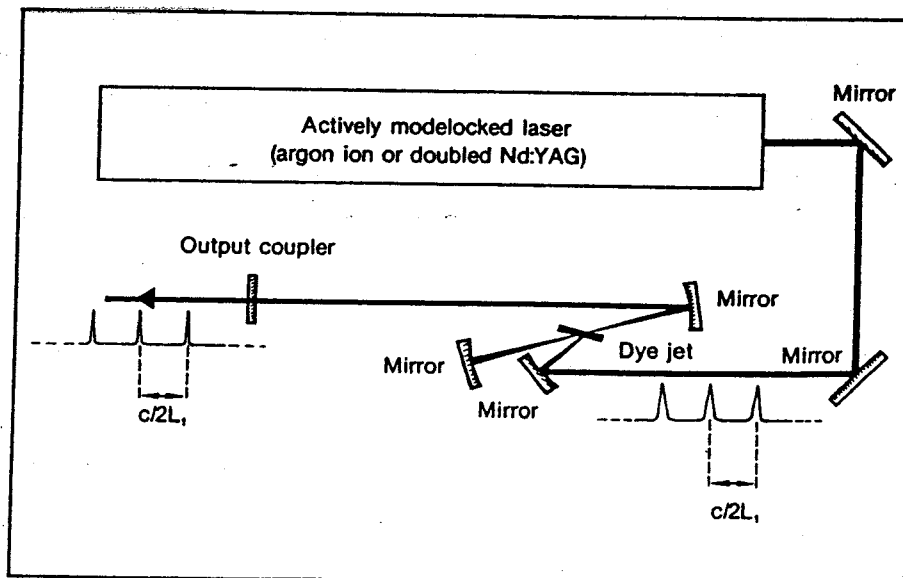


Figure 13. Schematic of a synchronously pumped modelocked dye laser.

the optimum cavity length.

Figure 15a depicts what happens when the cavity is longer than optimum. Lengthening the cavity retards the dye pulse, moving it further out in the gain curve past the point where the gain curve and loss line intersect. Because of the larger value of the unsaturated gain, the peak intensity of the pulse increases. At the same time, the pulse broadens to match the cavity round trip time with the period of the pump pulse. After reaching a maximum, the peak intensity of the pulse decreases for large cavity detuning (greater than $50\text{ }\mu\text{m}$) because of the loss of unsaturated gain by spontaneous emission. Increasing the cavity length ultimately precludes complete modelocking; the characteristic "Prussian helmet" shape of the autocorrelation traces appears in the dye pulse.

In contrast, if the laser cavity is shortened from the optimum position (Figures 15c and 15d), the dye pulse moves closer to the point where the gain crosses the loss line. The peak intensity of the pulse decreases because of the lower net gain experienced, and the pulse duration slightly decreases to fulfill the pump laser timing requirements. If the gain depletion induced by the dye pulse occurs early enough, the amplifier medium (which continues

integrating the pump pulse) can recover enough gain to overcome the cavity losses. This gain recovery allows the formation of a second pulse in the laser cavity, delayed by several tens of picoseconds from the main pulse. Further length reduction decreases the delay between the two pulses and can even lead to the generation of a third or fourth pulse in the laser cavity (Figure 15e). If the laser cavity is shortened until the dye pulse arrives before the gain curve crosses the loss line, the pulse is quenched. Lasing continues, however, in the form of a broadband pulse whose parameters are determined by the pump pulse and the saturation characteristics of the gain medium.

Thus, pulse structure is critically dependent on the adjustment of cavity length. For example, a Rhodamine 6G dye laser using a three-plate birefringent filter as a tuning element, when synchronously pumped by a modelocked, large-frame ion laser, displays the entire shape evolution depicted in Figure 15 for a total length variation of only $130\text{ }\mu\text{m}$.

The regime of "good modelocking" of a synchronously pumped system can be difficult to identify. Qualitatively, it can be arrived at by producing a pulse like that shown in Figure 15b, experimentally reduc-

ing the pulse width until just before a second pulse appears. For a dye laser producing a 6-ps pulse obtained with a three-plate birefringent filter, cavity length can only vary by about $10\text{ }\mu\text{m}$. Where single-plate birefringent filters are used to generate subpicosecond pulses, the corresponding requirement on the length adjustment falls below $1\text{ }\mu\text{m}$.

To generate subpicosecond pulses from a synchronously pumped dye laser, one must suppress the second pulse. Two methods have been advanced for suppressing the second pulse. The methods are not exclusive and have been simultaneously demonstrated in a commercial system.¹⁷

As noted earlier, the second pulse arises because of gain recovery after the passage of the first pulse. If the system is made to work close enough to threshold, the gain cannot overcome the losses after depletion. A given system can then be characterized by a critical value of its intracavity power at the dye medium; the critical value is that level above which a second pulse would be created under the required length condition. One means of accomplishing this task¹⁸ is to use a larger beam waist at the dye medium, to keep the critical power density below that needed to generate the second pulse. This design re-

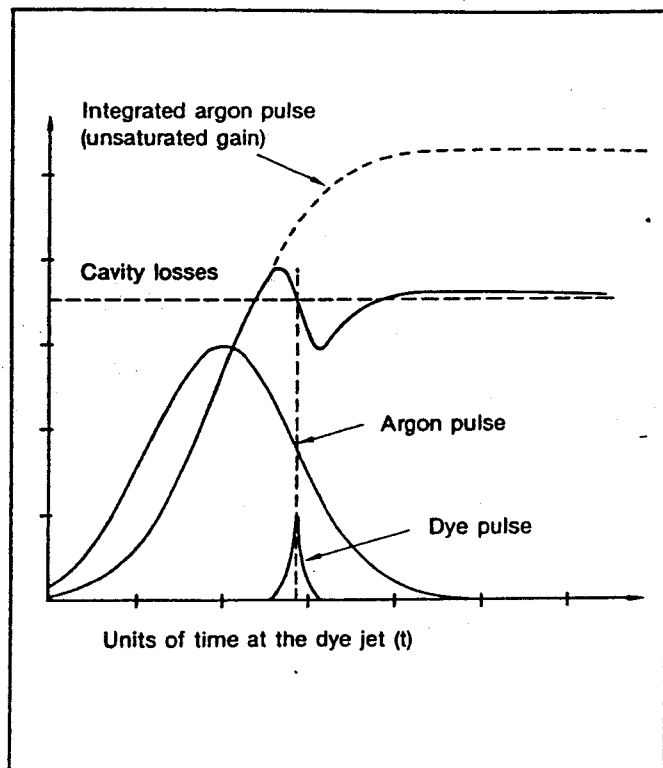


Figure 14. Schematic of the time variation of the gain, G , due to the passage of the pump and dye pulses through the dye jet. The evolution of the gain in the absence of the dye pulse is indicated by the dashed line. The situation represented corresponds to a dye cavity shorter than optimal, thus allowing the formation of a second pulse.

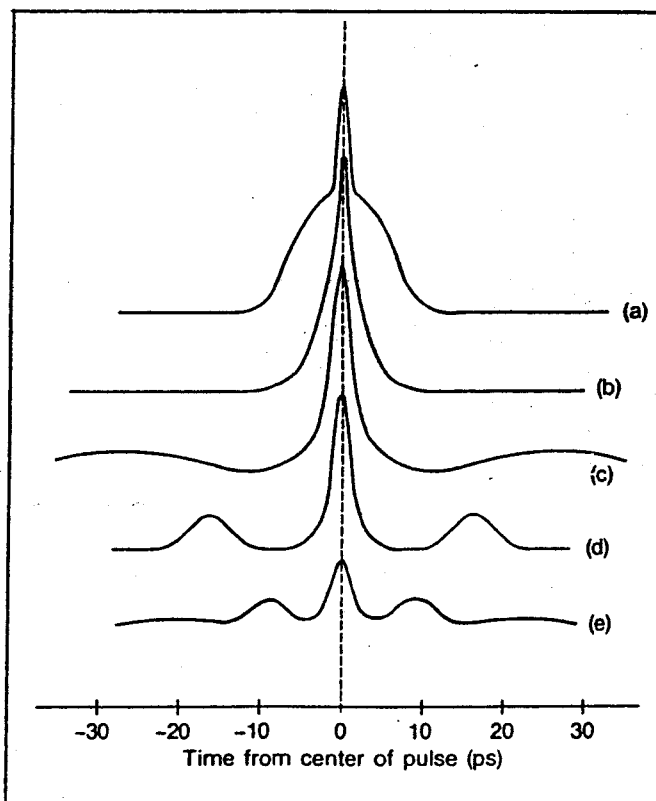


Figure 15. Autocorrelation traces of pulses obtained from a dye laser containing a three-plate birefringent filter. Each curve corresponds to a different cavity length. The dye laser cavity length has been decreased from longer than optimal (a) to shorter than optimal (e).

Table 1 — Comparison of Modelocking Techniques

Modelocking Technique	Laser Type	Modelocking Device	Typical Pulse Duration (ps)	Typical Pulse Energy (nJ)	Advantages	Disadvantages
Active	Ion Nd:YAG	Acousto-optic modelocker with RF driver	80 to 100 100 at 1.06 μm 70 at 532 nm	10 100 to 150 at 1.06 μm 10 to 15 at 532 nm	• Reliability • Ease of use • Stability • Low jitter • Reproducibility	• Need ultrastable RF generator and high-quality acousto-optic modulator with no transverse acoustic modes (shear modes)
Passive	Dye Nd:YAG	Saturable absorber	< 1	0.5	• Low cost (does not need modelocker) • Short pulses	• Low energy per pulse • Amplitude and phase noise
Synchronous pumping	Dye Color-center	Modelocked pump laser plus cavity length matching	Several	1 to 2	• Ease of use • Tunability • Short pulses • Can be cavity dumped	• Secondary pulses when ultrashort pulses are needed
Hybrid	Dye	Synchronous pumping saturable absorber	~0.5	1	• Same as for synchronous pumping, but with pulses one order of magnitude shorter	• For optimum performance, dye and absorber must be separated, so two jets and circulators are needed. • Saturable absorber concentration needs to be adjusted for large wavelength changes
CPM	Dye	Passive modelocking in ring cavity	<0.1	0.5	• Shortest pulse generated so far	• No cavity dumping • Low output power • Little or no tunability • Very critical optics

tains a good conversion efficiency for the system.

The second method is called hybrid modelocking and involves the placement of a saturable absorber in the synchronously pumped cavity.¹⁹ The action of the saturable absorber is twofold: It prevents the formation of the second pulse and contributes to an additional shortening of the main pulse. Both actions occur by the processes described earlier.

A condition for passive modelocking operation of a dye laser is that the saturable absorber saturates before the amplifier medium. This condition can be readily obtained if the power density is made larger at the saturable absorber than at the amplifier medium, by using two separate dye jets within the dye laser optical cavity.

Conclusion

Table 1 compares different modelocking techniques. We have included, for completeness, the colliding pulse modelocking technique, even though it is not described in this article. It will be part of a subsequent article. □

References

1. D.H. Auston, *IEEE J. of Quant. Elect.*, **QE-4**:420 (1968).
2. M.H. Crowell, *IEEE J. of Quant. Elect.*, **QE-1**:12 (1965).
3. R.H. Pantell and H.E. Puthoff, eds., *Fundamentals of Quantum Electronics*, John Wiley and Sons, New York.
4. P.W. Smith, *Proc. of the IEEE*, **58**:1342 (1970).
5. M.F. Becker, D.J. Kuizenga, and A.E. Siegman, *IEEE J. of Quant. Elect.*, **QE-8**:687 (1972).
6. L.E. Hargrove, R.L. Fork, and M.A. Pollock, *Appl. Phys. Lett.*, **5**:4 (1964).
7. O.P. McDuff and S.E. Harris, *IEEE J. of Quant. Elect.*, **QE-3**:101 (1967).
8. S.E. Harris and R. Targ, *Appl. Phys. Lett.*, **8**:180 (1966).
9. S.E. Harris and O.P. McDuff, *IEEE J. of Quant. Elect.*, **QE-1**:245 (1965).
10. D.J. Kuizenga and A.E. Siegman, *IEEE J. of Quant. Elect.*, **QE-6**:709 (1970).
11. H.W. Mocker and R.J. Collins, *Appl. Phys. Lett.*, **7**:270 (1965).
12. A.J. DeMaria, D.A. Stetser, and H. Heynau, *Appl. Phys. Lett.*, **8**:174 (1966).
13. H.A. Haus, *IEEE J. of Quant. Elect.*, **QE-11**:736 (1975).
14. N.J. Frigo, T. Daly, and H. Mahr, *IEEE J. of Quant. Elect.*, **QE-13**:101 (1977).
15. C.P. Ausschnitt, R.K. Jain, and J.P. Heritage, *IEEE J. of Quant. Elect.*, **QE-15**:912 (1979).
16. A. Scavennec, *Opt. Comm.*, **17**:14 (1976).
17. Model 700 Coherent Inc., Palo Alto CA.
18. J. Kluge, D. Wiechert, and D. Von der Linde, *Opt. Comm.*, **45**:278 (1983).
19. J.P. Ryan, L.S. Goldberg, and D.J. Bradley, *Opt. Comm.*, **27**:127 (1978).

Reprinted from
Lasers & Applications
January, 1985, Pages 79-83
February, 1985, Pages 91-94